Creating Oscillons and Oscillating Kinks in Two Scalar Field Theories

R. A. C. Correa^{a,b} *, A. de Souza Dutra^{c†}, T. Frederico^{b‡}, Boris A. Malomed^{d§}, O. Oliveira^{e¶}, N. Sawado^{f**}

Scuola Internazionale Superiore di Studi Avanzati (SISSA), via Bonomea, 265, I-34136 Trieste, Italy
ITA-Instituto Tecnológico de Aeronáutica, 12228-900, São José dos Campos, SP, Brazil
São Paulo State University (UNESP), Campus de Guaratinguetá, 12516-410, Guaratinguetá, SP, Brazil
Department of Physical Electronics, School of Electrical Engineering, Faculty of Engineering,
and Center for Light-Matter Interaction, Tel Aviv University, Tel Aviv 69978, Israel
CFisUC, Department of Physics, University of Coimbra, P-3004 516 Coimbra, Portugal
Department of Physics, Tokyo University of Science, Noda, Chiba 278-8510, Japan

Oscillons are time-dependent, localized in space, extremely long-lived states in nonlinear scalar-field models, while kinks are topological solitons in one spatial dimension. In the present work, we show new classes of oscillons and oscillating kinks in a system of two nonlinearly coupled scalar fields in 1+1 spatiotemporal dimensions. The solutions contain a control parameter, the variation of which produces oscillons and kinks with a flat-top shape. The model finds applications to condensed matter, cosmology, and high-energy physics.

Keywords:

*rafal.couceiro@sissa.it
†alvaro.dutra@unesp.br
‡tobias@ita.br
§malomed@post.tau.ac.il
¶orlando@uc.pt
**sawadoph@rs.tus.ac.jp

INTRODUCTION

Nonlinear field theories are commonly used in Physics to model phenomena at all energy scales [1], in condensed matter [2], in quantum solitons [3], in cosmology [4], in particle physics [8–10], and in other areas of physics [5–7]. One of fundamental reasons for the increasing interest in nonlinear phenomena is the possibility to have multiple degenerate minimum-energy configurations of the system. A good testbed to study the dynamics associated with the presence of degenerated minima are scalar field models whose potential energy has two or more degenerate minima. The present work addresses this topic, focusing in a particular model.

In nonlinear classical-field theories, solitons [11, 12] are localized field configurations with finite energy density, that keep their shape unaltered after collision with other solitons. These type of configurations have been studied in a wide class of contexts, such as nonlinear lattices [13], Skyrmion models [14, 15], theories breaking Lorentz invariance [16, 17], and the Maxwell-Chern-Simons gauge model [18].

The scalar nonlinear field theories allow for various types of configurations and, among then, are spatially localized time-periodic states named oscillons. Oscillons were discovered by Bogolyubsky and Makhankov [19] and rediscovered *a posteriori* by Gleiser [20]. Typically, they have bell-shaped profiles that oscillates sinusoidally in time [21, 22]. Further, oscillons are states in non-integrable models that continuously loose energy via radiation losses [24] but, nevertheless, can be represented by extremely long-lived modes and preserve the

self-trapping in the respective models [25]. These properties are not shared with other classes of solutions of nonlinear scalar field theories that the breathers of the one-dimensional sine-Gordon equations [23] are an example..

A vast body of results have been published for oscillons. In particular, they have been investigated in the presence of external potentials [26], in string-inspired cosmological models [27], in the context of supersymmetry [28], in perturbed sign-Gordon models [29], and in higher-derivative field theories [30]. Oscillons have also been studied in connection with gravitational waves [30–32], Abelian-Higgs models [33], in the context of the standard $SU(2) \times U(1)$ theory for electroweak interactions [34], and in theories probing violation of the Lorentz and CPT symmetries [41, 42].

An interesting scenario where oscillons can play a fundamental role is after cosmic inflation [35–38] as they act as a source of gravitational waves [39] and lead to a reduction in the uncertainties in the predictions for inflationary observables [40].

Oscillons configurations were not studied in detail in models with two or more interacting scalar fields. In this context, it was pointed out in Ref. [43] that a hybrid inflation model with two real scalar fields, interacting quadratically, can produce oscillon configurations whose lifetimes are much larger than those associated with single-field oscillons. As shown in that work, such configurations persist for at least four cosmological expansion times, accounting for up to 20% of the total energy density of the early Universe.

The oscillons solutions in theories with two scalar fields were also addressed in Ref. [44] in the framework of the dynamics of the Abelian Higgs model. By using a multiscale expansion method [45], a class of oscillons and oscillating kinks was obtained for both Higgs and gauge fields. Moreover, it was argued that similar dynamics occurs in superconductors and in the superfluid phase of atomic Bose-Einstein condensates trapped in optical lattices. Furthermore, in the framework of a similar sce-

nario it was shown [46] that it is possible to classify oscillons solutions according to their mass ratio and, accordingly, they may correspond to type-I or type-II superconductors. Various fluxon states produced by a system of sine-Gordon equations modelling a triangular configuration of three coupled long Josephson junctions were reported in Ref. [47]. It is also relevant to mention that it was recently shown [48–50] that cosmological backgrounds based on models with more than one scalar field accurately comply with constraints inferred from data collected by the Planck satellite.

The aim of the present work is to show that oscillons naturally emerge in a system of two nonlinearly coupled scalar fields in $(1+1)$-dimensional spatiotemporal continuum. We address a class of sixth-degree polynomial potentials, which allows for rich structure of vacua [51, 52]. This model also plays an important role in the description of topological twistons in polyethylene [53–55] and has also been used to investigate topological defects in molecular chains with zig-zag [56] and helix [57] structures. Unlike the oscillons and oscillating kinks considered in Refs. [44, 46], where solutions were produced by an effective nonlinear Schrödinger equation, herein we use the expansion procedure developed in Ref. [21] to construct two new classes of oscillons and two classes of oscillating kinks. In particular, it will be shown that oscillating-kink solutions include both single- and double-kink modes, and oscillons exhibit both bell-shaped and flat-top profiles.

This paper is organized as follows. In Section 2 we introduce the models with two interacting scalar fields. In Section 3 the method used for constructing oscillons solutions is presented. Then, new classes of oscillons and oscillating kinks are reported in Section 4, and their applications are discussed in Section 5. The work is concluded in Section 6.

THE TWO-SCALAR-FIELDS MODEL

Scalar field models with more than one scalar field naturally emerge in the study of many physical systems. Systems with two interacting scalar fields, that we address here, appear as models of networks of BPS (Bogomol'nyi-Prasad-Sommerfeld) and non-BPS defects [58], are used to describe fermion localization on degenerate and critical Bloch branes [59, 60], on the hierarchy problems [61], and in field-theory kinks [62].

Here, we aim to construct oscillons and related states in a two-component system that is close to one considered in Ref. [51]. The $(1 + 1)$-dimensional model includes a sixth-degree polynomial potential,

$$V(\phi, \chi) = \kappa_1 \phi^2 + \kappa_2 \chi^2 + \kappa_3 \phi^4 + \kappa_4 \chi^4 + \kappa_5 \phi^6$$
$$+ \kappa_6 \chi^6 + \kappa_7 \phi^2 \chi^2 + \kappa_8 \phi^2 \chi^4 + \kappa_9 \phi^4 \chi^2, \quad (1)$$

where $\phi = \phi(x, t)$ and $\chi = \chi(x, t)$ are real scalar fields, and κ_i are real coupling constants. Note that with the

choice of

$$\kappa_1 = \kappa_2 = \frac{\nu^2}{2}, \ \kappa_3 = \mu\nu, \ \kappa_4 = \lambda\nu,$$

$$\kappa_5 = \frac{\mu^2}{2}, \ \kappa_6 = \frac{\lambda^2}{2}, \kappa_7 = 3\nu(\lambda + \mu), \quad (2)$$

$$\kappa_8 = \frac{3\lambda}{2}(3\lambda + 2\mu), \ \kappa_9 = \frac{3\mu}{2}(3\mu + 2\lambda),$$

$V(\phi, \chi)$ reproduces the potential energy of the model introduced in [51],

$$V(\phi, \chi) = \frac{1}{2}\chi^2(\lambda\chi^2 + 3\mu\phi^2 + \nu)^2 + \frac{1}{2}\phi^2(3\lambda\chi^2 + \mu\phi^2 + \nu)^2$$
$$(3)$$

where λ, μ and ν are real positive coupling constants. This potential has a rich vacuum structure. For instance, for $\nu\lambda < 0$ and $\nu\mu < 0$ it has the following nine minima:

$$\mathcal{M}_1 = \Big(0, 0\Big),$$

$$\mathcal{M}_2 = \Big(-\sqrt{-\frac{\nu}{\mu}}, 0\Big),$$

$$\mathcal{M}_3 = \Big(\sqrt{-\frac{\nu}{\mu}}, 0\Big),$$

$$\mathcal{M}_4 = \Big(0, -\sqrt{-\frac{\nu}{\lambda}}\Big),$$

$$\mathcal{M}_5 = \Big(0, \sqrt{-\frac{\nu}{\lambda}}\Big), \quad (4)$$

$$\mathcal{M}_6 = \Big(-\sqrt{-\frac{\nu}{4\mu}}, -\sqrt{-\frac{\nu}{4\lambda}}\Big),$$

$$\mathcal{M}_7 = \Big(-\sqrt{-\frac{\nu}{4\mu}}, \sqrt{-\frac{\nu}{4\lambda}}\Big),$$

$$\mathcal{M}_8 = \Big(\sqrt{-\frac{\nu}{4\mu}}, -\sqrt{-\frac{\nu}{4\lambda}}\Big),$$

$$\mathcal{M}_9 = \Big(\sqrt{-\frac{\nu}{4\mu}}, \sqrt{-\frac{\nu}{4\lambda}}\Big).$$

where we used the notation $\mathcal{M}_n = (\phi, \chi)$ for two components of the n-th vacuum state.

The vacuum structure associated with potential (3) is sketched in Fig. 1, that also displays the potential's profile. One can predict different classical configurations by connecting different vacua.

Previous analysis of this model addressed only static field configurations, revealing several kink-like and lump-like solutions [51]. Our objective is to investigate solutions of the field equations that are time- and space-dependent.

SOLUTIONS OF THE COUPLED FIELD EQUATIONS

The two-component system is defined by the Lagrangian density,

$$\mathcal{L} = \frac{1}{2}(\partial_\alpha \phi)^2 + \frac{1}{2}(\partial_\alpha \chi)^2 - V(\phi, \chi), \quad (5)$$
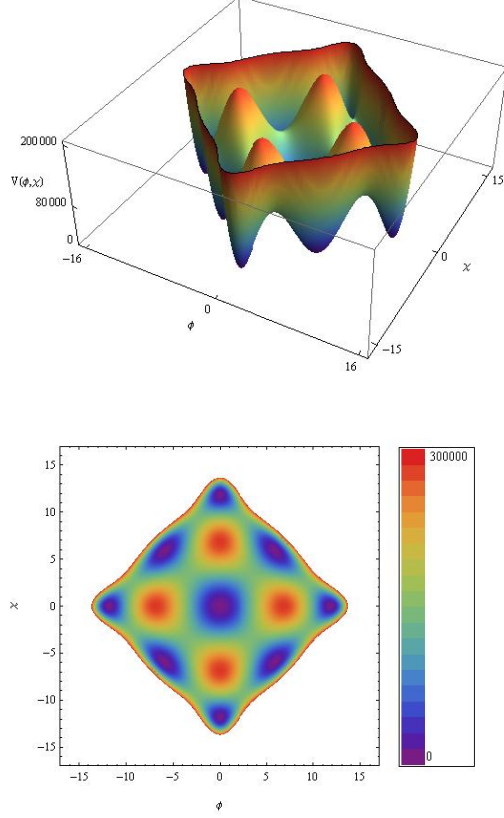
where ϵ is the same small parameter as in Eq. (8), and

$$\omega \equiv \sqrt{1 - \epsilon^2}. \qquad (10)$$

Such transformations naturally appear in the context of the multiscale expansion method [45], which defines several temporal and spatial variables, that are scaled differently and treated as independent ones.

Under the scale transformation (9), Eqs. (6) and Eq. (7), with the potential energy given in Eq. (1), become

$$(1 - \epsilon^2)\frac{\partial^2 \phi}{\partial \tau^2} - \epsilon^2 \frac{\partial^2 \phi}{\partial y^2} = -\left(2(\kappa_1 - \epsilon^2\delta^2)\phi \qquad (11)\right.$$
$$\left. + 4\kappa_3\phi^3 + 6\kappa_5\phi^5 + 2\kappa_7\phi\chi^2 + 4\kappa_9\phi^3\chi^2 + 2k_8\phi\chi^4\right),$$

$$(1 - \epsilon^2)\frac{\partial^2 \chi}{\partial \tau^2} - \epsilon^2 \frac{\partial^2 \chi}{\partial y^2} = -\left(2(\kappa_2 - \epsilon^2\delta^2)\chi \qquad (12)\right.$$
$$\left. + 4\kappa_4\chi^3 + 6\kappa_6\phi^5 + 2\kappa_7\phi^2\chi + 2\kappa_9\phi^4\chi + 4\kappa_8\phi^2\chi^3\right).$$

The standard approach used to obtain oscillons configurations is based on the expansion of the scalar fields as powers of ϵ. Given that Eqs. (11) and (12) are odd in the fields, the expansions defining ϕ and χ include only odd powers of ϵ:

$$\phi(y, \tau) = \sum_{n=1}^{\infty} \epsilon^{2n-1}\phi_{2n-1}(y, \tau), \qquad (13)$$

$$\chi(y, \tau) = \sum_{n=1}^{\infty} \epsilon^{2n-1}\chi_{2n-1}(y, \tau). \qquad (14)$$

Then, Eqs. (11) and (12) yield

$$\epsilon\left(\frac{\partial^2 \phi_1}{\partial \tau^2} + 2\kappa_1\phi_1\right) + \epsilon^3\left(\frac{\partial^2 \phi_3}{\partial \tau^2} + 2\kappa_1^2\phi_3 - \frac{\partial^2 \phi_1}{\partial \tau^2}\right.$$
$$\left. -\frac{\partial^2 \phi_1}{\partial y^2} - 2\delta^2\phi_1 + 4\kappa_3\phi_1^3 + 2\kappa_7\phi_1\chi_1^2\right) + \mathcal{O}(\epsilon^5) = 0,$$
$$(15)$$

$$\epsilon\left(\frac{\partial^2 \chi_1}{\partial \tau^2} + 2\kappa_2\chi_1\right) + \epsilon^3\left(\frac{\partial^2 \chi_3}{\partial \tau^2} + 2\kappa_2\chi_3 - \frac{\partial^2 \chi_1}{\partial \tau^2}\right.$$
$$\left. -\frac{\partial^2 \chi_1}{\partial y^2} - 2\delta^2\chi_1 + 4\kappa_4\chi_1^3 + 2\kappa_7\phi_1^2\chi_1\right) + \mathcal{O}(\epsilon^5) = 0.$$
$$(16)$$

In the two lowest orders, Eqs. (15) and (16) lead to the

FIG. 1: The profile of potential $V(\phi, \chi)$ (top) and vacuum states (botton) produced by Eq. (3) with constants $\lambda = \mu = 1$ and $\nu = -140$.

with $V(\phi, \chi)$ given by Eq. (3). We use a system of units such that $c = \hbar = 1$, the metric is $\eta_{\alpha\beta} = \text{diag}(1, -1)$, and the coordinates are $x^\alpha = (t, x)$. The classical equations of motion generated by $\mathcal{L}$ are

$$\frac{\partial^2 \phi(x, t)}{\partial t^2} - \frac{\partial^2 \phi(x, t)}{\partial x^2} + \frac{\partial V(\phi, \chi)}{\partial \phi} = 0, \qquad (6)$$

$$\frac{\partial^2 \chi(x, t)}{\partial t^2} - \frac{\partial^2 \chi(x, t)}{\partial x^2} + \frac{\partial V(\phi, \chi)}{\partial \chi} = 0. \qquad (7)$$

A small perturbation will be added to potential (1) as a means for creating time-dependent configurations. A simple way to introduce the perturbation is to replace

$$\kappa_{1,2} \to \kappa_{1,2} - \delta^2\epsilon^2 \qquad (8)$$

in Eq. (1), where $\epsilon << 1$ is a small parameter, while δ is a generic coefficient (it is required in this definition as the same small parameter ϵ is introduced below in another context, see Eqs. (9) and (10)).

Our main objective is to find very long-lived spatially localized time-dependent configurations, using an appropriate procedure devised in Ref. [21]. As a first step, x and t are rescaled as

$$\tau = \omega\, t, \qquad y = \epsilon\, x, \qquad (9)$$

following set of coupled nonlinear differential equations:

$$\frac{\partial^2 \phi_1}{\partial \tau^2} + 2\kappa_1 \phi_1 = 0, \tag{17}$$

$$\frac{\partial^2 \chi_1}{\partial \tau^2} + 2\kappa_2 \chi_1 = 0, \tag{18}$$

$$\frac{\partial^2 \phi_3}{\partial \tau^2} + 2\kappa_1 \phi_3 = \frac{\partial^2 \phi_1}{\partial \tau^2} + \frac{\partial^2 \phi_1}{\partial y^2} \tag{19}$$
$$+2\delta^2 \phi_1 - 4\kappa_3 \phi_1^3 - 2\kappa_7 \phi_1 \chi_1^2,$$

$$\frac{\partial^2 \chi_3}{\partial \tau^2} + 2\kappa_2 \chi_3 = \frac{\partial^2 \chi_1}{\partial \tau^2} + \frac{\partial^2 \chi_1}{\partial y^2} \tag{20}$$
$$+2\delta^2 \chi_1 - 4\kappa_4 \chi_1^3 - 2\kappa_7 \phi_1^2 \chi_1.$$

Equations (17) and (18) are of the harmonic-oscillator type, hence their solution can be written as

$$\phi_1(y,\tau) = \varphi(y) \cos(\sqrt{2\kappa_1}\tau), \tag{21}$$

$$\chi_1(y,\tau) = \sigma(y) \sin(\sqrt{2\kappa_2}\tau). \tag{22}$$

Functions $\varphi(y)$ and $\sigma(y)$, i.e. the spatial profile of the configurations appearing in Eqs. (21) and (22), can be obtained inserting $\phi_1(y,\tau)$ and $\chi_1(y,\tau)$ in Eqs. (19) and (20). After straightforward manipulations, one gets

$$\frac{\partial^2 \phi_3}{\partial \tau^2} + 2k_1\phi_3 =$$
$$-\left(2(\kappa_1 - \delta^2)\varphi + 3\kappa_3\varphi^3 + \kappa_7\varphi\sigma^2 - \frac{d^2\varphi}{dy^2}\right)\cos(\sqrt{2\kappa_1}\tau)$$
$$-\varphi(\kappa_3\varphi^2 - \frac{\kappa_7}{2}\sigma^2)\cos(3\sqrt{2\kappa_1}\tau), \tag{23}$$

$$\frac{\partial^2 \chi_3}{\partial \tau^2} + 2k_2\chi_3 =$$
$$-\left(2(\kappa_2 - \delta^2)\sigma + 3\kappa_4\sigma^3 + k_7\varphi^2\sigma - \frac{d^2\sigma}{dy^2}\right)\sin(\sqrt{2\kappa_2}\tau)$$
$$+\sigma(\kappa_4\sigma^2 - \frac{\kappa_7}{2}\varphi^2)\sin(3\sqrt{2\kappa_2}\tau). \tag{24}$$

For field configurations that are periodic in time, the contribution proportional to $\cos(\sqrt{2\kappa_1}\tau)$ and $\sin(\sqrt{2\kappa_2}\tau)$ in the right-hand side of Eqs. (23) and (24) must vanish, otherwise solutions of the equations produced by these *resonant* driving terms will generate a term linear in τ, hence the solutions for ϕ_3 and χ_3 will be not be time-periodic ones. This condition translates into the equations

$$\frac{d^2\varphi}{dy^2} = 2(\kappa_1 - \delta^2)\varphi + 3\kappa_3\varphi^3 + \kappa_7\varphi\sigma^2, \tag{25}$$

$$\frac{d^2\sigma}{dy^2} = 2(\kappa_2 - \delta^2)\sigma + 3\kappa_4\sigma^3 + k_7\varphi^2\sigma, \tag{26}$$

that determine $\varphi(y)$ and $\sigma(y)$. In general, nonlinear equations (25) and (26) are quite difficult to solve. However, as shown in the next section, they can be mapped into first-order linear differential equations whose general solution can be constructed by means of standard methods.

OSCILLONS AND OSCILLATING-KINK SOLUTIONS

Now, our goal is to reduce the second-order differential equations (25) and (26) to first-order ones. To this end, we write these equations as

$$\frac{d^2\varphi}{dy^2} = U_\varphi(\varphi,\sigma), \qquad \frac{d^2\sigma}{dy^2} = U_\sigma(\varphi,\sigma), \tag{27}$$

where

$$U_\varphi(\varphi,\sigma) \equiv 2(\kappa_1 - \delta^2)\varphi + 3\kappa_3\varphi^3 + \kappa_7\varphi\sigma^2, \tag{28}$$

$$U_\sigma(\varphi,\sigma) \equiv 2(\kappa_2 - \delta^2)\sigma + 3\kappa_4\sigma^3 + k_7\varphi^2\sigma. \tag{29}$$

To decouple the pair of Eqs. (27), we multiply the first and second equation by $d\sigma/dy$ and $d\varphi/dy$, respectively, and take their sum, to arrive at the result

$$\frac{1}{2}\left[\left(\frac{d\varphi}{dy}\right)^2 + \left(\frac{d\sigma}{dy}\right)^2\right] + U(\varphi,\sigma) = \alpha_0. \tag{30}$$

Here α_0 is an arbitrary constant, that should be set equal to zero to get solutions that connect different vacua of the system, and $U(\varphi,\sigma)$ is an effective potential that can be written, using a supersymmetric representation for function $U(\varphi,\sigma)$ in terms of a *superpotential*, $\mathcal{W}(\varphi,\sigma)$, as

$$U(\varphi,\sigma) = \frac{1}{2}[\mathcal{W}_\varphi^2(\varphi,\sigma) + \mathcal{W}_\sigma^2(\varphi,\sigma)], \tag{31}$$

where subscripts stand for derivatives with respect to φ and σ, and the appropriate superpotential is

$$\mathcal{W}(\varphi,\sigma) = -a_1\varphi + \frac{b_1}{3}\varphi^3 + c_1\varphi\sigma^2, \tag{32}$$

with the following definitions

$$a_1 \equiv \sqrt{\frac{2(\delta^2 - \kappa_2)(3\delta^2 - \kappa_1 - \kappa_2)}{\kappa_7}}, \tag{33}$$

$$b_1 \equiv (\delta^2 - \kappa_1)\sqrt{\frac{\kappa_7}{2(\delta^2 - \kappa_2)(3\delta^2 - \kappa_1 - \kappa_2)}}, \tag{34}$$

$$c_1 \equiv (\delta^2 - \kappa_2)\sqrt{\frac{\kappa_7}{2(\delta^2 - \kappa_2)(3\delta^2 - \kappa_1 - \kappa_2)}}. \tag{35}$$

It follows from Eqs. (33)-(35) that, to produce real solutions, the constants should be subject to the following restrictions:

$$\delta^2 < \kappa_1, \qquad \delta^2 > (\kappa_1 + \kappa_2)/3, \qquad \kappa_7 < 0, \qquad \kappa_3 = \kappa_4. \tag{36}$$

The advantage of this transformation is that it is possible to reduce the second-order differential equations (27) to first-order ones,

$$\frac{d\varphi}{dy} = \mathcal{W}_\varphi, \qquad\qquad \frac{d\sigma}{dy} = \mathcal{W}_\sigma. \qquad (37)$$

Following Ref. [64], one obtains from Eq. (37) an equation for φ considered as a function of σ:

$$\frac{d\varphi}{d\sigma} = \frac{\mathcal{W}_\varphi}{\mathcal{W}_\sigma} = \frac{b_1(\varphi^2 - 1) + c_1\sigma^2}{2c_1\varphi\sigma}. \qquad (38)$$

In terms of variable $\rho \equiv \varphi^2 - 1$, Eq. (38) is cast in the form of a linear ODE,

$$\frac{d\rho}{d\sigma} - \frac{b_1\rho}{c_1\sigma} = \sigma, \qquad (39)$$

whose general solution is

$$\rho(\sigma) = c_0\sigma^{b_1/c_1} - \frac{c_1}{b_1 - 2c_1}\sigma^2, \qquad (b_1 \neq 2c_1) \quad (40)$$

$$\rho(\sigma) = \sigma^2[\ln(\sigma) + d_1], \qquad (b_1 = 2c_1), \qquad (41)$$

where c_0 and d_1 are arbitrary integration constants. Next, these solutions feed the first-order ODE for σ in Eq. (37), that become

$$\frac{d\sigma}{dy} = \pm 2\, b_1\, \sigma\, \sqrt{1 + c_0\sigma^{b_1/c_1} - \frac{c_1}{b_1 - 2c_1}\sigma^2}, \quad (42)$$
$$\text{for } (b_1 \neq 2c_1),$$

$$\frac{d\sigma}{dy} = \pm 2\, b_1\, \sigma\, \sqrt{1 + \sigma^2[\ln(\chi) + d_1]}, \qquad (43)$$
$$\text{for } (b_1 = 2c_1).$$

As shown in ref. [64], Eq. (42) can be solved analytically, at least, for four different particular combinations of constants. Moreover, requiring that the solutions remain globally finite implies that c_0 cannot exceed some critical values. Therefore, borrowing the solutions from Ref. [64], one can write the corresponding classical field, at order ϵ, for the following cases:

A1. For $c_0 < -2$ and $b_1 = c_1$,

$$\phi_A^{(1)}(y,\tau) = \epsilon\left[\frac{\left(\sqrt{c_0^2 - 4}\right)\sinh(2c_1 y)}{\left(\sqrt{c_0^2 - 4}\right)\cosh(2c_1 y) - c_0}\right] \times,$$
$$\cos(\sqrt{2\kappa_1}\tau) + \mathcal{O}(\epsilon^3), \qquad (44)$$

$$\chi_A^{(1)}(y,\tau) = \epsilon\left[\frac{2}{\left(\sqrt{c_0^2 - 4}\right)\cosh(2c_1 y) - c_0}\right] \times$$
$$\sin(\sqrt{2\kappa_2}\tau) + \mathcal{O}(\epsilon^3). \qquad (45)$$

A2. For $b_1 = 4c_1$ and $c_0 < 1/16$,

$$\phi_A^{(2)}(y,\tau) = \epsilon\left[\frac{\left(\sqrt{1 - 16c_0}\right)\sinh(4c_1 y)}{\left(\sqrt{1 - 16c_0}\right)\cosh(4c_1 y) + 1}\right] \times$$
$$\cos(\sqrt{2\kappa_1}\tau) + \mathcal{O}(\epsilon^3), \qquad (46)$$

$$\chi_A^{(2)}(y,\tau) = \epsilon\left[-\frac{2}{\sqrt{\left(\sqrt{1 - 16c_0}\right)\cosh(4c_1 y) + 1}}\right] \times$$
$$\sin(\sqrt{2\kappa_2}\tau) + \mathcal{O}(\epsilon^3). \qquad (47)$$

B1. For $b_1 = c_1$ and $c_0 = -2$,

$$\phi_B^{(1)}(y,\tau) = \epsilon\left[-\frac{1}{2}\left[\tanh(c_1 y) \mp 1\right]\right] \times \qquad (48)$$
$$\cos(\sqrt{2\kappa_1}\tau) + \mathcal{O}(\epsilon^3),$$

$$\chi_B^{(1)}(y,\tau) = \epsilon\left[\frac{1}{2}\left[1 \pm \tanh(c_1 y)\right]\right] \times \qquad (49)$$
$$\sin(\sqrt{2\kappa_2}\tau) + \mathcal{O}(\epsilon^3).$$

B2. For $b_1 = 4c_1$ and $c_0 = 1/16$,

$$\phi_B^{(2)}(y,\tau) = \epsilon\left[\frac{1}{2}\left[\pm 1 - \tanh(2c_1 y)\right]\right] \times \qquad (50)$$
$$\cos(\sqrt{2\kappa_1}\tau) + \mathcal{O}(\epsilon^3),$$

$$\chi_B^{(2)}(y,\tau) = \epsilon\left[\sqrt{2}\,\frac{\cosh(c_1 y) \pm \sinh(c_1 y)}{\sqrt{\cosh(2c_1 y)}}\right] \times \quad (51)$$
$$\sin(\sqrt{2\kappa_2}\tau) + \mathcal{O}(\epsilon^3).$$

The solutions of types A1 – B2 are illustrated in Figs. 2 and 3 that display the ϕ and χ components for solutions of type $A1$ and a particular set of the parameters, as indicated in the figure caption. The solutions in the ϕ component interpolate at $|y| \to \infty$ between different vacua of the classical-field potential. Their spatial profiles look like kinks in the ϕ^4 theory, hence we call them oscillating kinks. The localized χ components will be called oscillating lumps.

The displayed examples demonstrate that the system with two scalar fields admits approximate solutions that oscillate with time, with the ϕ component keeping the oscillating kink-like profile, while the χ component features the oscillating lump-shape. Note that in all the families of solutions, the presence of a nonvanishing arbitrary parameter c_1 is necessary for the emergence of a flat segment in the lump (the χ field) and double-kink structure in the ϕ component.

EMISSION OF RADIATION

As shown in the seminal work by Segur and Kruskal [65] (see also Ref. [66]), one-dimensional oscillons very slowly decay through emission of small-amplitude radiation waves. In this section we compute the outgoing radiation of the oscillons and oscillating kinks, by means
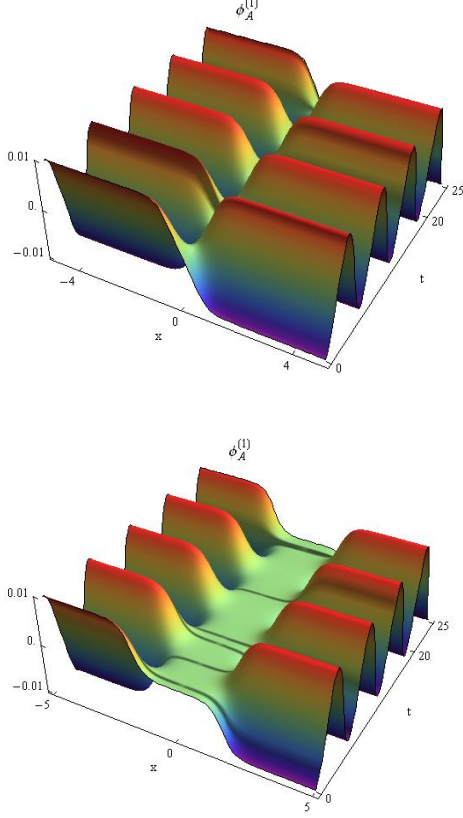
FIG. 2: Oscillating kinks computed for $\lambda = \mu = -1$, $\nu = 1$, $\epsilon = 0.01$ and $\delta = 0.6$. Note that we are using the potential from Eq. (3), whose parameters are related to those in Eq. (1) by the relations defined in Eq. (??). The top and bottom figures show the solutions, respectively, for $c_0 = -2.1$ and $c_0 = -2.00001$.

FIG. 3: Oscillon configurations for the same parameters as in the top and bottom panels of Fig. 2.

of a method similar to the one elaborated by Hertzberg [67] for a single scalar field. Here we extend it for systems with two scalar fields.

The method relies on writing the solutions of the classical field equations in the following form:

$$\phi_{\rm osc}(x,t) = \phi_{\rm kink}(x,t) + \xi_{\rm rad}(x,t), \qquad (52)$$
$$\chi_{\rm sol}(x,t) = \chi_{\rm osc}(x,t) + \zeta_{\rm rad}(x,t), \qquad (53)$$

where $\phi_{\rm osc}$ and $\chi_{\rm sol}$ are the oscillating-kink and oscillon solutions, respectively, while, $\xi_{\rm rad}$ and $\zeta_{\rm rad}$ represents small radiation components, which are generated by linearized equations following from the substitution of the decompositions (52) and (53) in Eqs. (6) and (7):

$$\Box\xi_{\rm rad} + \Gamma_\xi \xi_{\rm rad} = -j_\xi(x,t), \qquad (54)$$
$$\Box\zeta_{\rm rad} + \Gamma_\zeta \zeta_{\rm rad} = -j_\zeta(x,t), \qquad (55)$$

where $\Box$ stands the usual D'Alembertian operator, $\Gamma_\xi \approx 2\kappa_1$ and $\Gamma_\zeta \approx 2\kappa_2$, and the radiations sources are written as
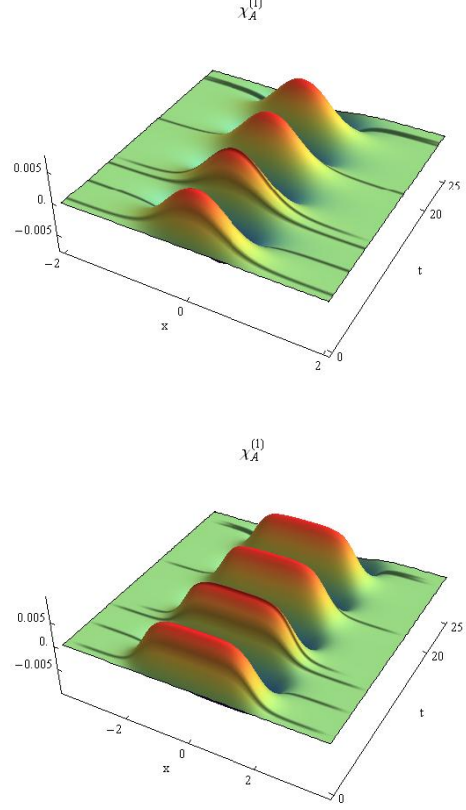
$$j_\xi(x,t) = \epsilon^3 \kappa_3 \varphi^3 \cos(3\omega\sqrt{2\kappa_1}t) + ..., \qquad (56)$$
$$j_\zeta(x,t) = \epsilon^3 \kappa_4 \sigma^3 \sin(3\omega\sqrt{2\kappa_2}t) + ... \,. \qquad (57)$$

Following the approach developed in Ref. [67], we can write the radiation fields in the form

$$\xi_{\rm rad}(x,t) = -\frac{1}{(2\pi)^2} \int\int dK d\Omega \times \qquad (58)$$
$$\frac{j_\xi(K,\Omega)}{K^2 - \Omega^2 + 1 \pm i0^+} e^{i(Kx-\Omega t)},$$
$$\zeta_{\rm rad}(x,t) = -\frac{1}{(2\pi)^2} \int\int dK d\Omega \times \qquad (59)$$
$$\frac{j_\zeta(K,\Omega)}{K^2 - \Omega^2 + 1 \pm i0^+} e^{i(Kx-\Omega t)}.$$

In the above equation, $j_\xi(K,\Omega)$ and $j_\zeta(K,\Omega)$ are the Fourier transforms of $j_\xi(x,t)$ and $j_\zeta(x,t)$. Then, after straightforward manipulations, we obtain

$$\xi_{\text{rad}}(x,t) = -\frac{\epsilon^3 \kappa_3}{8\pi^2 \sqrt{\bar{n}_1^2 - \Gamma_\xi}} \cos(K_{\text{rad}}^{(1)} x + \Delta_1) \times \quad (60)$$
$$\cos(\bar{n}_1 t) j_\xi(K_{\text{rad}}^{(1)}),$$

$$\zeta_{\text{rad}}(x,t) = -\frac{\epsilon^3 \kappa_4}{8\pi^2 \sqrt{\bar{n}_2^2 - \Gamma_\zeta}} \cos(K_{\text{rad}}^{(2)} x + \Delta_2) \times \quad (61)$$
$$\sin(\bar{n}_2 t) j_\xi(K_{\text{rad}}^{(2)}),$$

where we define

$$\bar{n}_1 \equiv 3\omega\sqrt{2\kappa_1}, \;\; K_{\text{rad}}^{(1)} \equiv \sqrt{\bar{n}_1^2 - \Gamma_\xi}, \qquad (62)$$

$$\bar{n}_2 \equiv 3\omega\sqrt{2\kappa_2}, \;\; K_{\text{rad}}^{(2)} \equiv \sqrt{\bar{n}_2^2 - \Gamma_\zeta}, \qquad (63)$$
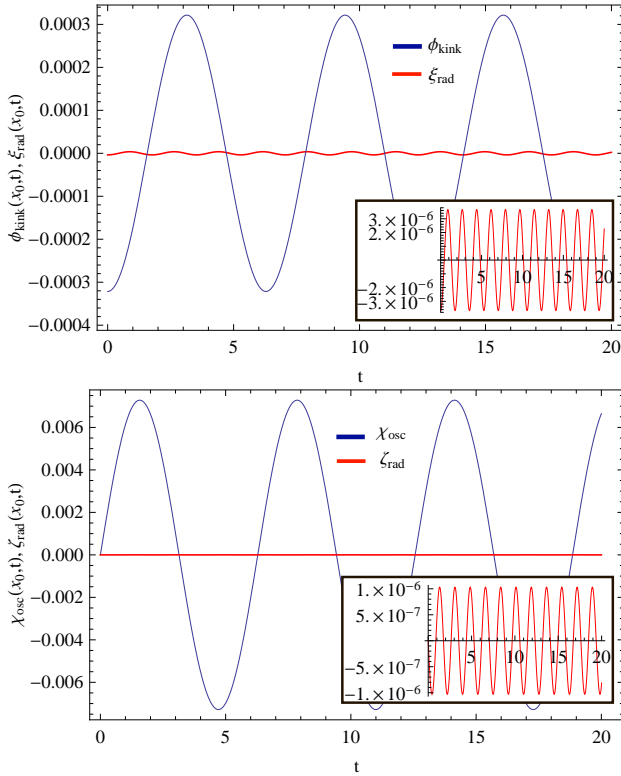
and Δ_1 and Δ_2 being phase constants.

FIG. 4: The amplitude of the outgoing radiation determined by the Fourier transform for solutions with $b_1 = c_1$ and with $c_0 < -2$. The top and bottom plots shows the solutions computed with $c_0 = -2.1$. Potential (3) is used here, with $\lambda = \mu = -1$, $\nu = 1$, $\epsilon = 0.01$ and $\delta = 0.6$.

In Fig. (4) we show how the amplitudes of the outgoing radiation vary in time, being, indeed, very small in comparison with the amplitudes of the underlying oscillating kink and oscillating-lump modes. Furthermore, we also examined how the outgoing radiation vary in time for the configurations corresponding to Eqs. (46) and (47), concluding that the qualitative picture remain the same.

It has been checked by means of long simulations (see below) that the solutions classified above as A1 an A2 are completely stable. On the other hand, the solutions of the B1 type are unstable, and B2 are partially stable. Namely, in solutions B1 both components are unstable, while in B2 the field ϕ collapses very fast, while component χ is a long-standing one. Thus, it is concluded that B1 solutions decay very fast after their creation, and in B2 the two-field configuration rapidly evolves into a long-lived single-field oscillon, while the A1 and A2 species are truly long-lived oscillating patterns.

NUMERICAL RESULTS

To check the above analytical results, numerical solutions have been produced for the oscillons and oscillating kinks. To this end, Eqs. (6) and (7) were solved with initial conditions

$$\phi_{\text{num}}^{(1)}(x,0) = \epsilon \frac{\left(\sqrt{c_0^2 - 4}\right)\sinh(2c_1 \epsilon x)}{\left(\sqrt{c_0^2 - 4}\right)\cosh(2c_1 \epsilon x) - c_0}, \quad (64)$$

$$\chi_{\text{num}}^{(1)}(x,0) = \epsilon \frac{2}{\left(\sqrt{c_0^2 - 4}\right)\cosh(2c_1 \epsilon x) - c_0}, \quad (65)$$

which correspond to coefficients $b_1 = c_1$, see Eqs. (34) and (35), and $c_0 = -2.1$. To illustrate the field configurations produced by the simulations for oscillating kinks and oscillons, in Fig. (5) we plot fields $\phi(x,t)$ and $\chi(x,t)$ at $x = 0.5$. The figure, as well as additional numerical results, not shown here, demonstrate good agreement of the analytical solutions with their numerical counterparts.

SUMMARY AND CONCLUSIONS

In the present work we have investigated solutions of a system of two nonlinearly coupled scalar fields in the one-dimensional space, with a multiple vacuum structure. The analysis shows that systems of this type has a rich dynamics. In particular, we were able to determine new classes of time-dependent solutions, in the form of oscillatory kinks and lump oscillons. As far as we know, the existence and dynamics of oscillons and kinks in models with two scalar fields were previously addressed only in Ref. [44]. However, in that work only solutions with states of the same type (kinks or lumps) in both components were considered, while here we investigate solutions combining oscillatory kinks and lumps in the two components. In our case, we have found that some of them are stable (types A1 and A2), while others (B1 and B2) are not. Despite the spatial interpolation of the classical vacua of the theory, it is not clear if these type of solutions are stable and are representative solutions of different topological sectors for the Manifold of the classical solutions of the field equations. Indeed, the fact that the
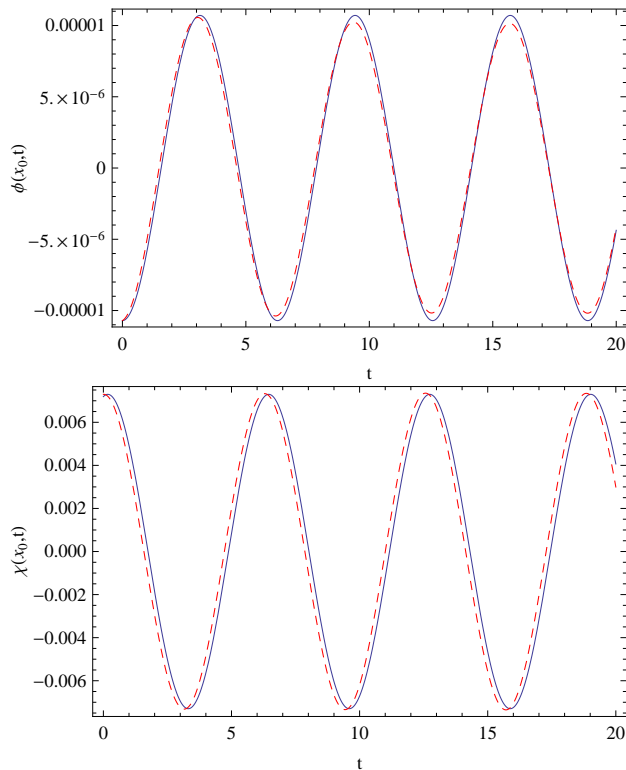
FIG. 5: Comparison of the analytical and numerical results for $b_1 = c_1$ and $c_0 = -2.1$ at point $x_0 = 0.5$, shown, respectively, by the solid and dashed curves. Here, potential (3) is used, with $\lambda = \mu = -1$, $\nu = 1$, $\epsilon = 0.01$ and $\delta = 0.6$.

oscillons being approximate solutions of the field equations also raise the question if their time evolution can lead to a classification of the classical field equations into topological sectors, a problem that we will address in a future work.

The new lump and kink oscillons configurations reported here may include relatively large flat regions, where the fields are essentially different from the vacuum values. Away from the central flat region, the solutions varying rapidly, approaching vacua values. Plotting the respective orbits in the (ϕ, χ) plane, see Fig. 3, one finds that the fields surround the vacuum point, featuring very small values, which is a typical behavior demonstrated by oscillons.

Our interest in the two-component system considered in this work is that it provides a relatively simple model with a rich vacuum structure, if compared to other theories with complex vacuum structures, such as gauge theories. Further, the model considered in the current work has applications to condensate matter, cosmology and high-energy physics. In particular, in the study of low-dimensional materials similar to graphene, scalar fields naturally appear as models of impurities and defects [68], and also model a carbon structure on the top of which the dynamics of the electrons occurs [69].
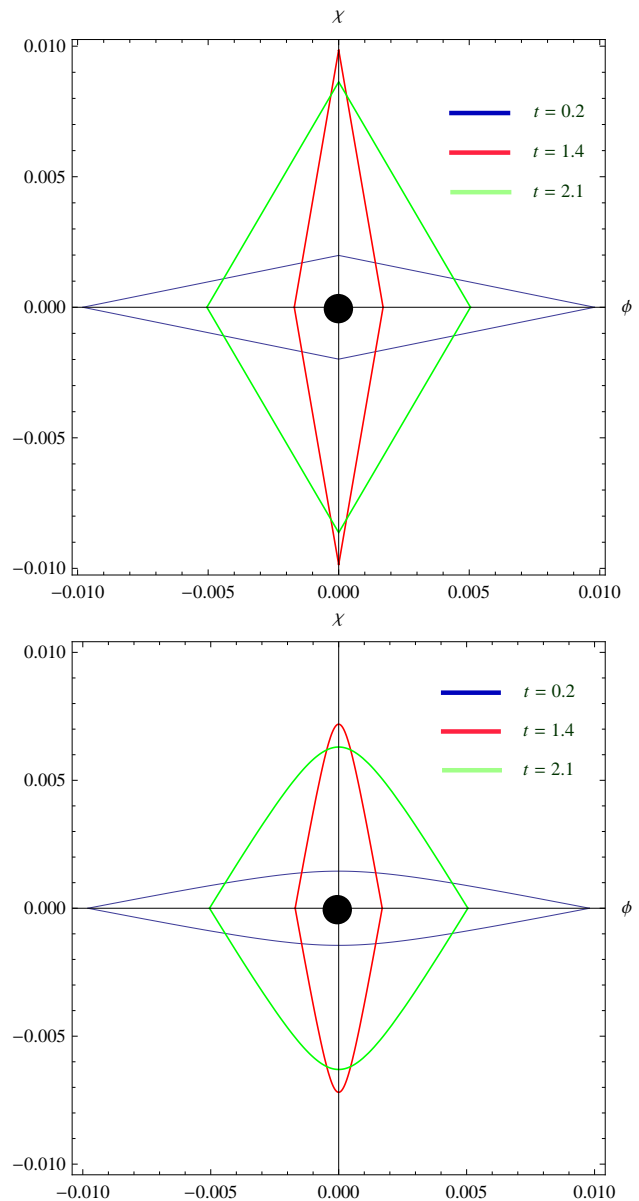

FIG. 6: Solutions in the (ϕ, χ) plane for solutions with $b_1 = c_1$ and vacuum state of the potential located at point $(0, 0)$. The top and bottom plots shows the solutions computed with $c_0 = -2.000001$ and $c_0 = -2.1$, respectively. As in Figs. 2 and 3, these solutions pertain to $\lambda = \mu = -1$, $\nu = 1$, $\epsilon = 0.01$ and $\delta = 0.6$.

1287/17.

———————

[1] E. J. Weinberg, *Classical Solutions in Quantum Field Theory: Solitons and Instantons in High Energy Physics*, Cambridge University Press, Cambridge, England, 2012.

[2] T. Yefsah, A. T. Sommer, M. J. H. Ku, L. W. Cheuk, W. Ji, W. S. Bakr, and M. W. Zwierlein, Nature **499** (2013) 426.

[3] T. Vachaspati, *Kinks and Domain Walls: An Introduction to Classical and Quantum Solitons*, Cambridge University Press, Cambridge, England, 2006.

[4] A. Vilenkin, E.P.S. Shellard, *Cosmic Strings and Other Topological Defects*, Cambridge University, Cambridge, England, 1994.

[5] Y. S. Kivshar and B. A. Malomed, Rev. Mod. Phys. **61** (1989) 763.

[6] B. Kibler, J. Fatome, C. Finot, G. Millot, F. Dias, G. Genty, N. Akhmediev, and J. M. Dudley, Nature Physics **6** (2010) 790.

[7] L. V. Yakushevich, A. V. Savin, and L. I. Manevitch, Phys. Rev. E **66** (2002) 016614.

[8] M. P. Bento, H. E. Haber, J. C. RomÃƒÂ£o and J. P. Silva, JHEP **1810**, 143 (2018) doi:10.1007/JHEP10(2018)143 [arXiv:1808.07123 [hep-ph]].

[9] S. Iguro, Y. Muramatsu, Y. Omura and Y. Shigekami, JHEP **1811**, 046 (2018) doi:10.1007/JHEP11(2018)046 [arXiv:1804.07478 [hep-ph]].

[10] N. Chakrabarty and I. Chakraborty, Int. J. Mod. Phys. A **34**, 1950025 (2019).

[11] N. J. Zabusky and M. D. Kruskal, Phys. Rev. Lett. **15** (1965) 240.

[12] R. Rajaraman, *Solitons and Instantons*, North-Holland, Amsterdam, 1982.

[13] Y. V. Kartashov, B. A. Malomed, and L. Torner, Rev. Mod. Phys. 83 (2011) 247.

[14] I. Perapechka, N. Sawado, and Y.Shnir, J. High Energ. Phys. **1810** (2018) 081.

[15] L. A. Ferreira and W. J. Zakrzewski, J. High Energy Phys. **1309** (2013) 097.

[16] A. de Souza Dutra and R. A. C. Correa, Phys. Rev. D **83** (2011) 105007.

[17] R. A. C. Correa, R. da Rocha, and A. de Souza Dutra, Annals Phys. **359** (2015) 198.

[18] A.Y. Loginov and V. V. Gauzshtein, Phys. Lett. B **784** (2018) 112.

[19] I. L. Bogolyubsky and V. G. Makhankov, Pis'ma v Zhurnal Eksperimental'noi i Teoreticheskoi Fiziki, **24** (1976) 15.

[20] M. Gleiser, Phys. Rev. D **49** (1994) 2978.

[21] G. Fodor, P. Forgács, Z. Horváth, and Á. Lukács, Phys. Rev. D **78** (2008) 025003.

[22] G. Fodor, P. Forgács, Z. Horváth, and M. Mezei, J. High Energy Phys. **0908** (2009) 106.

[23] G. Mussardo, *Statistical Field Theory: An Introduction to Exactly Solved Models in Statistical Physics*, Oxford University Press, New York. 2010.

[24] G. Fodor, P. Forgács, Z. Horváth, and M. Mezei, Phys. Rev. D **79** (2009) 065002.

[25] E. J. Copeland, M. Gleiser, and H. R. Muller, Phys. Rev. D **52** (1995) 1920. (1995).

[26] T. Romańczukiewicz and Y. Shnir, J. High Energy Phys. **1801** (2018) 101.

[27] S. Antusch, F. Cefala, S. Krippendorf, F. Muia, S. Orani and F. Quevedo, JHEP **1801** (2018) 083.

[28] R. A. C. Correa, L. P. R. Ospedal, W. de Paula, and J. A. Helayël-Neto, Phys.Lett. B **780** (2018) 159.

[29] P. Klimas, J. S. Streibel, A. Wereszczynski, and W. J. Zakrzewski, J. High Energy Phys. **1804** (2018) 102.

[30] J. Sakstein and M. Trodden, Phys.Rev. D **98** (2018) 123512.

[31] M. A. Amin, J. Braden, E. J. Copeland, J. T. Giblin, C. Solorio, Z. J. Weiner and S. Y. Zhou, Phys. Rev. D **98** (2018) 024040.

[32] S. Antusch, F. Cefala and S. Orani, JCAP **1803** (2018) no.03, 032.

[33] M. Gleiser and J. Thorarinson, Phys. Rev. D **79** (2009) 025016.

[34] N. Graham, Phys.Rev.Lett. **98** (2007) 101801.

[35] K. D. Lozanov and M. A. Amin, Phys. Rev. D **90** (2014) 083528.

[36] K. D. Lozanov and M. A. Amin, JCAP **1606** (2016) no.06, 032.

[37] K. D. Lozanov and M. A. Amin, Phys. Rev. Lett. **119** (2017) no.6, 061301.

[38] K. D. Lozanov, A. Maleknejad and E. Komatsu, JHEP **1902** (2019) 041.

[39] K. D. Lozanov and M. A. Amin, Phys. Rev. D **99** (2019) no.12, 123504

[40] K. D. Lozanov and M. A. Amin, Phys. Rev. D **97** (2018) no.2, 023533.

[41] R. A. C. Correa and A. de Souza Dutra, Adv. High Energy Phys. **2015** (2015) 673716.

[42] R. A. C. Correa, R. da Rocha, and A. de Souza Dutra, Phys. Rev. D **91** (2015) 125021.

[43] M. Gleiser, N. graham, and N. Stamatopoulos, Phys. Rev. D **83** (2011) 096010.

[44] V. Achilleos, F. K. Diakonos, D. J. Frantzeskakis, G. C. Katsimiga, X. N. Maintas, E. Manousakis, C. E. Tsagkarakis, and A. Tsapalis, Phys. Rev. D **88** (2013) 045015.

[45] A. Jeffrey and T. Kawahara, *Asymptotic methods in nonlinear wave theory*, Pitman, London, 1982.

[46] F. K. Diakonos, G. C. Katsimiga, X. N. Maintas, and C. E. Tsagkarakis, Phys. Rev. E **91** (2015) 023202.

[47] S. P. Yukon and B. A. Malomed, J. Math. Phys. **56** (2015) 091509.

[48] J. Ellis, M. Fairbairn, and M. Sueiro, JCAP **02** (2014) 044.

[49] R. Easther, J. Frazer, H.V. Peiris, L.C. Price, Phys. Rev. Lett. **112** (2014) 161302.

[50] L. C. Price, H. V. Peiris, J. Frazer, and R. Easther, Phys. Rev. Lett. **114** (2015) 031301.

[51] L. E. Arroyo Meza, A. de Souza Dutra, J. R. L. dos Santos, M. B. Hott1, and O. C. Winter, Eur. Phys. Lett. **98** (2012) 10011.

[52] G. P. de Brito and A. de Souza Dutra, Phys. Lett. B **736** (438) 2014.

[53] D. Bazeia and E. Ventura, Chem. Phys. Lett. **303** (1999) 341.

[54] D. Bazeia, E. Ventura,and A. Simas, Chem. Phys. Lett. **320** (2000) 587.

[55] A. de Souza Dutra, J. R. L. dos Santos, and O. C. Winter, J. Phys A **43** (2010) 365402.

[56] A. V. Zolotaryuk, P. L. Christiansen, and A. V. Savin, Phys. Rev. E **54** (1996) 3881.

[57] A. V. Zolotaryuk, P. L. Christiansen, and A. V. Savin, Phys. Rev. E **56** (1997) 877.

[58] D. Bazeia, F. A. Brito, Phys. Rev. D **61** (2000) 105019.

[59] D. Bazeia and A. R. Gomes, J. High Energy Phys. **0405** (2004) 012.

[60] R. A. C. Correa, A. de Souza Dutra, and M. B. Hottt, Class. Quant. Grav. **28** (2011) 155012.

[61] A. de Souza Dutra, G. P. de Brito, and J. M. Hoff da Silva, Eur. Phys. Lett. **108** (2014) 11001.

[62] A. A. Izquierdo, M. A. Gonzalez Leon, and J. Mateos Guilarte, Phys. Rev. D **65** (2002) 085012.

[63] D. Bazeia, L. Losano, and J. M. C. Malbouisson, Phys. Rev. D **66** (2002) 101701.

[64] A. de Souza Dutra, Phys. Lett. B **626** (2005) 249.

[65] H. Segur and M. D. Kruskal, Phys. Rev. Lett. **58** (1987) 747.

[66] Yu. S. Kivshar and B. A. Malomed, Phys. Rev. Lett. **60** (1988) 164.

[67] M. P. Hertzberg, Phys. Rev. D **82** (2010) 045022.

[68] A. H. Castro Neto, F. Guinea, N. M. R. Peres, K. S. Novoselov and A. K. Geim, Rev. Mod. Phys. **81** (2009) 109.

[69] O. Oliveira, C. E. Cordeiro, A. Delfino, W. de Paula and T. Frederico, Phys. Rev. B **83**, (2011) 155419.